UCID--19672
DE84 002018

INITIAL TMX-U THERMAL-BARRIER EXPERIMENTS

T. C. Simonen, S. L. Allen, L. Berzins,
M. Carter, T. A. Casper, J. F. Clauser,
C. A. Clower, F. H. Coensgen, D. L. Correll,
W. F. Cummins, C. C. Damm, B. H. Failor,
S. Falabella, M. Flammer, J. H. Foote,
R. K. Goodman, D. P. Grubb, D. N. Hill,
E. B. Hooper, R. S. Hornady, A. L. Hunt,
W. L. Hsu, R. A. James, R. G. Kerr, C. Lasnier,
G. W. Leppelmeier, J. M. Moller, A. W. Molvik,
T. J. Nash, W. E. Nexsen, W. L. Pickles,
P. Poulsen, B. W. Stallard, J. Taska,
W. C. Turner, and T. L. Yu

October 5, 1983

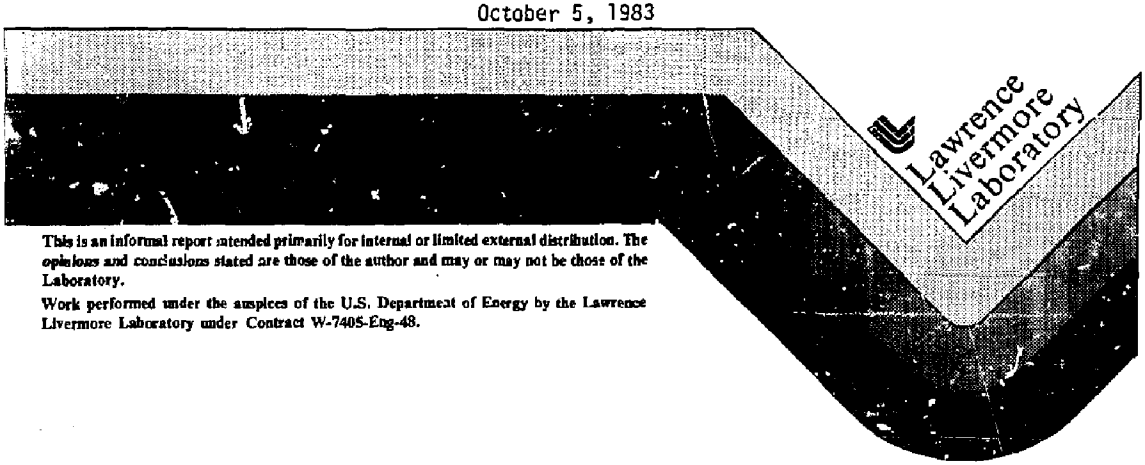

INITIAL TMX-U THERMAL-BARRIER EXPERIMENTS

T. C. Simonen, S. L. Allen, L. Berzins, M. Carter, T. A. Casper, J. F. Clauser, C. A. Clower, F. H. Coensgen, D. L. Correll, W. F. Cummins, C. C. Damm, B. H. Failor, S. Falabella, M. Flammer, J. H. Foote, R. K. Goodman, D. P. Grubb, D. N. Hill, E. B. Hooper, R. S. Hornady, A. L. Hunt, W. L. Hsu,* R. A. James,† R. G. Kerr, C. Lasnier,† G. W. Leppelmeier, J. M. Moller, A. W. Molvik, T. J. Nash, W. E. Nexsen, W. L. Pickles, P. Poulsen, B. W. Stallard, J. Taska, W. C. Turner, and T. L. Yu**

Lawrence Livermore National Laboratory, University of California
Livermore, California 94550 U.S.A.

ABSTRACT

This paper describes results from the initial thermal barrier experiments in the Tandem Mirror Experiment-Upgrade (TMX-U). Strong end plugging has been produced using a combination of ECRH gyrotrons with sloshing ion beam injection. Plugging has been achieved with a central cell higher than that of the end plugs. In these low-density central cell experiments (7×10^{11} cm^{-3}) the axial losses ($\tau_{\parallel}$ = 20 to 80 ms) are smaller than the radial losses ($\tau_{\perp}$ = 4 to 8 ms). Although no direct measurements are yet available to determine if a thermal barrier potential dip is generated, these experiments support many theoretical features of the thermal barrier concept.

*Sandia National Laboratory, Livermore, CA 94550
**Johns Hopkins University, Baltimore, MD 21218
†University of Maryland, College Park, MD 20742

I. EXECUTIVE SUMMARY

Early TMX-U experiments at low density have shown very encouraging results. Potential enhancement driven by ECRH has been demonstrated and shown to produce strong end plugging. The facts that end plugging requires both ECRH and sloshing ions, and that end plugging can be generated with central cell densities exceeding end plug densities, strongly supports the thermal barrier concept, as outlined in TABLE I. However, no direct measurements are yet available to determine if a thermal barrier potential depression is generated.

This report describes results of the initial TMX-U thermal barrier experiments. Previously we reported results from sloshing ion [1] and hot mirror-confined electron experiments.[2] The parameters of these initial thermal barrier experiments are listed in TABLE II. The major difference between the achieved parameters and our goal is that the present experiments operate at low central cell density and temperature. Subsequent experiments will progress to higher densities and temperatures with central cell ICRH, with an increased efficiency ECRH waveguide system, and with an improved gas feed system.

II. INTRODUCTION

The Tandem Mirror Experiment-Upgrade (TMX-U) [3] was built to investigate the tandem mirror thermal barrier [4] concept. Thermal barriers improve end plug ion microstability and allow the generation of higher electrostatic confining potentials to increase central cell ion confinement.

As indicated in Fig. 1, in the earlier TMX standard tandem experiment [5-7] central cell electrostatic confining potential ϕ_c was generated by a high density end plug [8,9]

$$\phi_c = T_e \ell n \frac{n_p}{n_c} \quad , \tag{1}$$

TABLE 1. Thermal barrier characteristics.

	TMX-U observation
1. End plugging with $n_c > n_p$	Yes
2. Potential peak enhanced by ECRH	Yes
3. Rapid rise of end loss when plug gyrotron is turned off	Yes
4. End plugging requires both sloshing ions and plug ECRH	Yes
5. Improved axial confinement	Yes
6. Ion microstability	Yes
7. Plug density from central cell decoupled	Yes
8. Potential dip between end plug and central cell	No data yet available
9. Non-Maxwellian plug electrons. End plug electron "temperature" exceeds central cell temperature	No data yet available

TABLE II. TMX-U plasma parameters: June 1983 and (proposal).

	End plug				Central cell			
	Hot electrons		Sloshing ions		Warm ions		Beam injection	
Energy (keV)	30-70	(50)	5-10	(10)	0.1	(0.9)	5-10	(6)
Density (10^{12} cm^{-3})	1-2	(4)	0.5-3[a]	(2.5)	0.7-5[a]	(15)	2	(6)
Beta (%, average[b] perpendicular	3-5	(15)	1	(1)	-		8	(12)
Radius[b] (cm)	22-17	(15)	15-12	(14)	26	(20)	-	
Length (cm)	120	(60)	210	(210)	510	(445)	400	
Confinement time (ms)	20-40	(19)	3	(7)	4-8	(17)	5	(10)

( ) = proposal value predicted [3]

a = without hot electrons, sloshing ion mode

b = parabolic radial profile, $\hat{\beta} = 2 \langle\beta\rangle$

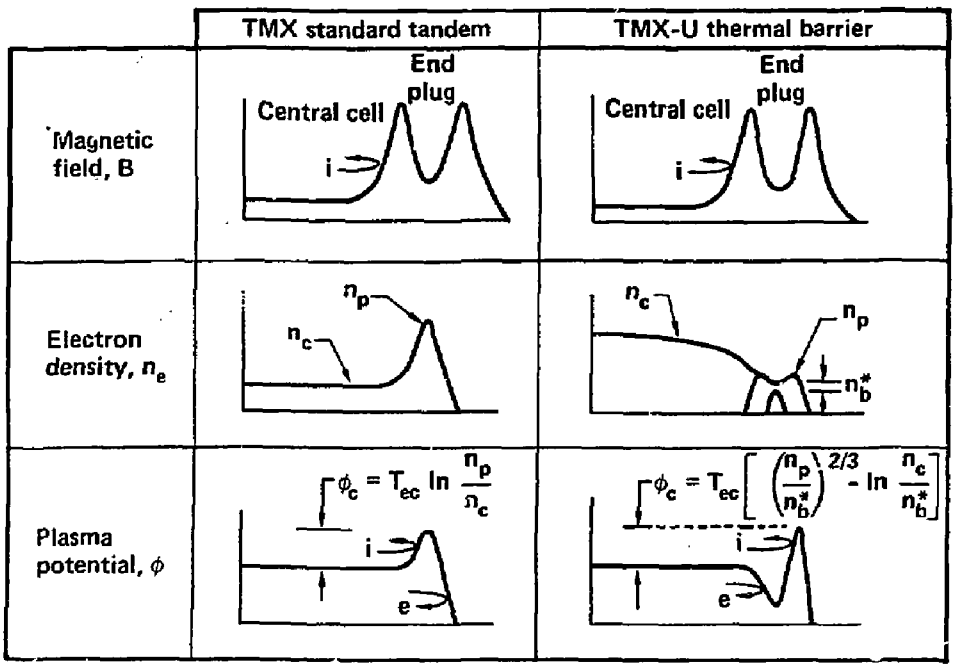

Figure 1. Schematic diagram of tandem mirror axial profiles.

where T_e is the electron temperature and n_p and n_c are the plug and central cell plasma densities. Low energy ions that are required for end plug ion microstability were supplied by leakage of central cell ions. However, when scaling the standard tandem mirror to a reactor, [10] the high end plug densities required to generate high-confining potentials lead to high-field minimum-B magnets and high energy neutral beams. In addition, supplying the low-energy ions for microstability lead to high power drain. These disadvantages are overcome in the thermal barrier tandem mirror.

In the thermal barrier concept microwave heating power is used to generate high potentials with low end plug densities. A potential peak off the plug midplane is driven by ECRH and supported by a density peak in magnetically trapped ions--in TMX-U beams are injected at the midplane at 47 deg to the magnetic axis. The potential dip at the end plug midplane reduces the microwave heating power needed to generate the potential peaks at the outside of each end plug by isolating the electrons in the potential peak from the cooler central cell electrons. Oblique injection, rather than the orthogonal used in TMX, improves the stability of the Alfven ion cyclotron (AIC) mode, which was the main microinstability observed in TMX. [11] The tipped potential allows low-energy central cell ions to be confined within the end plugs for microstability. Thus, these ions do not introduce an extra power drain.

The central cell confining potential depends on the strength of the microwave heating power. If the ECRH power is low, [8]

$$\phi_c = T_{ep} \ln \frac{n_p}{n_b^*} \left(\frac{T_{ec}}{T_{ep}}\right)^{1/2} - T_{ec} \ln \frac{n_c}{n_b^*} \quad , \tag{2}$$

where n_b^* is the non-mirror-confined electron density at the end cell midplane. Here we see the advantage of having a high density of mirror confined electrons (i.e., making n_b^* small). In this model the plug and central cell electron temperatures (T_{ep} and T_{ec}) are assumed to be Maxwellian. When the ECRH power is high, the electron distribution in the end plugs is strongly distorted from Maxwellian and the resulting confining potential is [12,13]

$$\phi_c/T_{ec} = \left(\frac{3}{4}\sqrt{\pi}\,\frac{R_{pb}-1}{R_{pb}}\,\frac{n_p}{n_b^*}\exp\left\{\phi_b/[T_{ec}\,(R_{mb}-1)]\right\}\right)^{2/3} - \ln\frac{n_c}{n_b^*} \quad . \tag{3}$$

Here R_{pb} is the mirror ratio from the potential peak to the barrier, R_{mb} is the mirror ratio of the inner mirror to the barrier, and ϕ_b is the potential drop from the central cell to the barrier minimum. Equation (3), which is derived in Ref. 12, reduces to an approximate form for TMX-U parameters,

$$\phi_c/T_{ec} = \frac{2}{3}\left(\frac{n_p}{n_b^*}\right)^{2/3}\left(\frac{n_c}{n_b^*}\right)^{1/5} - \ln\frac{n_c}{n_b^*} \quad . \tag{4}$$

The TMX-U experiment operates in the strong radio frequency limit described by Eq. (4).

A characteristic of mirror systems is that confinement improves at high temperatures. The consequence of this favorable behavior means that the temperature must be raised at low density and then the density increased. Alternatively, high-power startup heating systems could be employed to reach equilibrium confinement conditions.

In TMX-U we are following the low density startup approach outlined in Fig. 2 and TABLE III. This figure shows the axial profiles of magnetic field, density, and potential at each phase in the startup time sequence. First, hot electron density buildup begins at low density to accomodate the ECRH power requirement. When the source plasma temperature T_{ec} is low, collisional losses of rf trapped electrons are reduced if the source density n_{ec} is also low. As the hot electron end plug density builds up above that of the central cell, a small dip in potential must form to hold ions to charge-neutralize the mirror-confined electrons (see Fig. 2).

Sloshing beam injection is initiated once the hot electron line density is sufficiently high to trap the beams, approximately 10^{13} cm^{-2}. The sloshing ion density then builds up as in step 2 provided the cold gas density is sufficiently low compared to the sloshing beam atom density. Positive peaks must now develop to confine the electrons necessary to charge-neutralize the magnetically confined ions. Simultaneously the potential profile adjusts as in step 3 because the ECRH power boils electrons out of the outer potential peak.

The fourth and final step, not shown on Fig. 2, is to increase the density while maintaining the high temperature. The requirements outlined for this step in TABLE III suggest that ICRH can help [14] increase the central

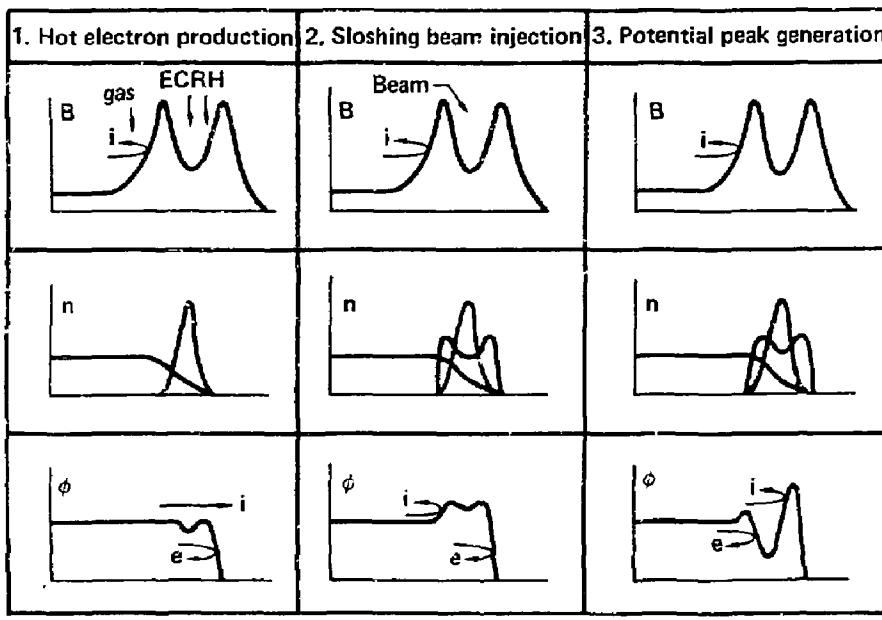

Figure 2. Schematic diagram of TMX-U thermal barrier startup sequence.

TABLE III. Thermal barrier startup sequence. The equipment and requirements of each proceeding step are necessary for each subsequent step.

Step	Equipment	Requirements
1. Hot electron production	ECRH, gas feed	Low n_{ec} for efficient rf trapping
2. Sloshing beam injection	Sloshing beams	$n_{gas} < n_{beam}$
3. Potential formation	As in 1 and 2	As in 1 and 2
4. High density buildup	Central cell gas puffing, Central cell ICRH, 18 deg pump beams, Central cell beams.	Barrier filling $\sim n_{ic}^2/T_{ic}^{3/2}$ $\int n_c dl > 10^{14}$ cm^{-2}

cell ion temperature T_{ic} at low density and that pump beams can help the sloshing beams pump out the thermal barrier. Once the central cell line density is sufficient (about 10^{14} cm^{-2}), neutral beam heating can augment ICRH and become the dominant source of central cell heating.

At present, the TMX-U experiments have progressed to step 3 and are beginning step 4. In the remaining sections of this report we describe our results during each of these startup phases.

III. EXPERIMENTAL RESULTS

When the ECRH-produced hot electrons [2,15] and beam-injected sloshing ions [1,16,17] are combined we observe strong end plugging. Results are shown in Fig. 3; they show very low end losses (3e) during the period when both ECRH (3a) and sloshing beams (3b) are operational. Also notice that, in this case, for single-ended running the end plug density is higher than that of the central cell.

That the end plugging requires sloshing ions is shown in Fig. 4. The injected sloshing beam current is modulated, and the end losses are similarly modulated. On closer examination we find stoppering begins 0.3 ms after sloshing-beam injection. This is the time required to accumulate a density of sloshing ions comparable to the central cell density. When the sloshing beams are turned off, the end losses increase on a 2-ms time scale, characteristic of the sloshing-ion lifetime.

There are two ECRH gyrotrons illuminating each end plug. The barrier ECRH gyrotron at 0.5 T primarily generates mirror confined electrons with a 20 to 40 ms lifetime (see Fig. 3). The end plugging gyrotron at 1.0 T generates the plugging potential and also produces warm electrons to feed the second-harmonic barrier ECRH. As shown in Fig. 5 the plugging ECRH is responsible for the reduction in ion end losses. Once the barrier ECRH creates the hot mirror-confined electrons it can be turned off, since the hot electrons are long lived.

A feature of end plugging in TMX-U, shown in Fig. 6, is that once the plugging ECRH power is off, the end losses rise very rapidly, in less than 1 ms. This is more rapidly than the plug or central cell densities change and, we believe, is due to the fact that the plugging potential is supported

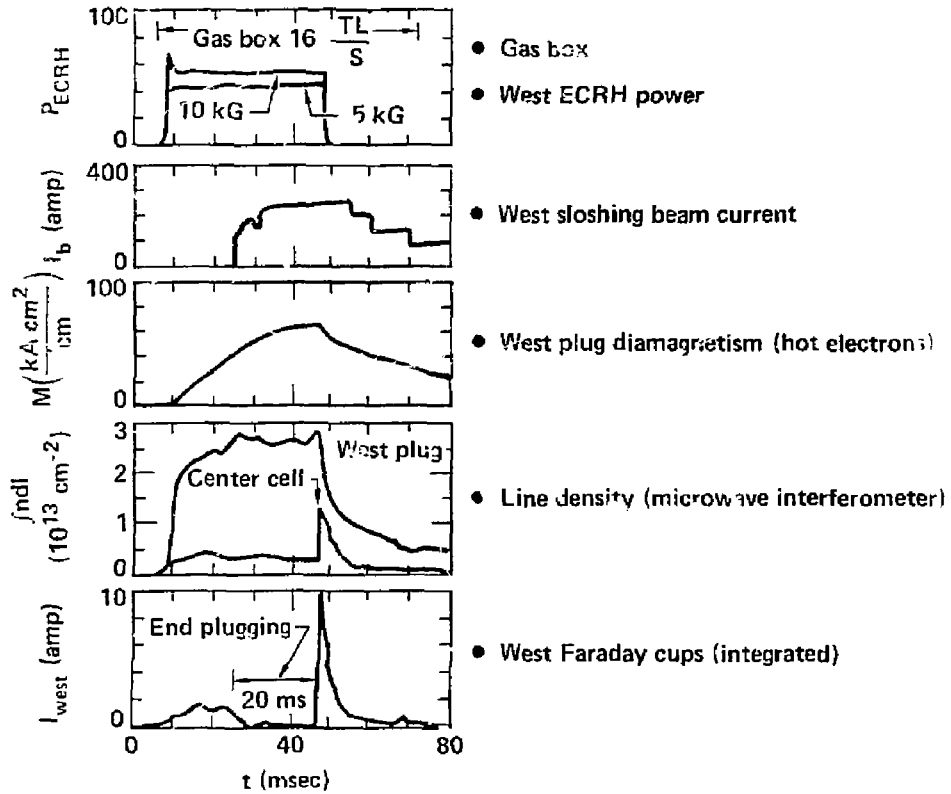

Figure 3. Demonstration of ECRH end plugging. Shown vs time is (a) ECRH power, (b) sloshing beam current, (c) hot-electron diamagnetism, (d) west plug and central cell microwave interferometer line density and, (e) west Faraday cup integrated ion end loss current.

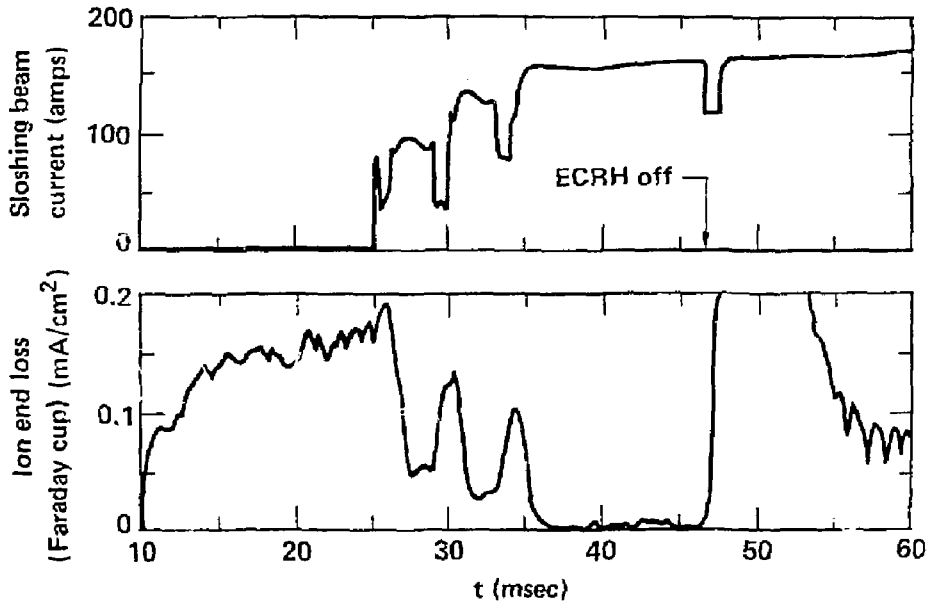

Figure 4. The ion end loss current density, shown vs time, is reduced when sloshing beam current is turned on, demonstrating that end plugging requires sloshing beams.

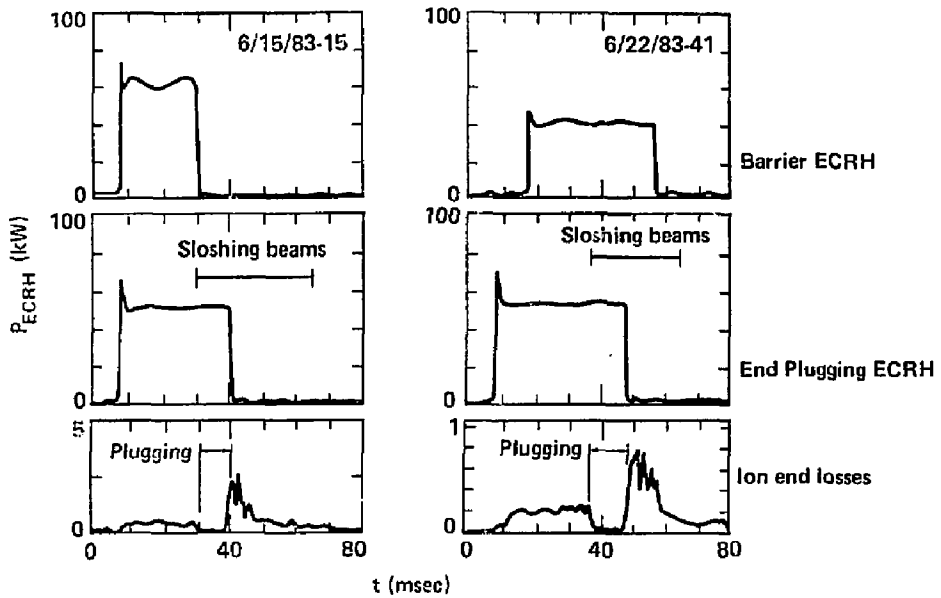

Figure 5. End plugging requires ECRH power at the potential peak. Shown vs time is (a) the barrier ECRH power, (b) the end plugging ECRH power and (c) the ion end loss current.

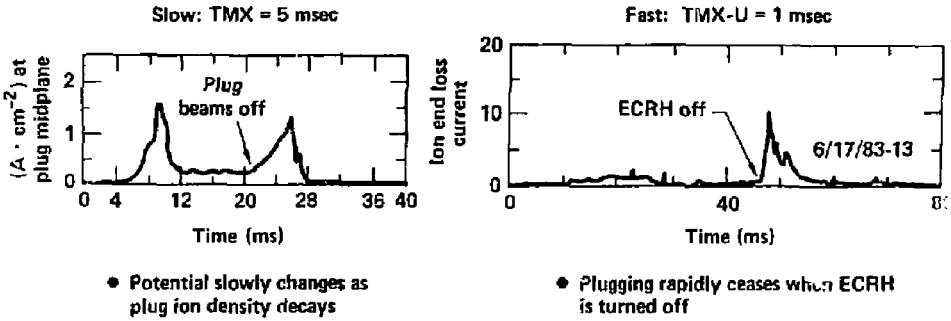

Figure 6. A comparison of TMX and TMX-U end loss rate of rise after end plug turn off.

by the non-Maxwellian electron distribution function. The potential can therefore decrease on the electron relaxation time scale. In contrast, in TMX the end losses rise more slowly, on the 3- to 5-ms time scale required for the end plug density to decay. This provides further evidence that TMX-U end plugging occurs by thermal barrier type ECRH potential enhancement rather than by conventional tandem mirror plugging.

These experiments were operated with only one end plug. Consequently we could determine the end plug and central cell potential with end loss analyzers on each end wall. These measurements, shown in Fig. 7, indicate that during strong plugging, confining potentials of 0.6 kV are generated. This is twice the best achieved in our previous TMX experiments. We have not yet measured whether a thermal barrier depression in potential exists.

In addition to single-ended end plugging we have also plugged up both ends, as shown in Fig. 8. In this case both ends were plugged for 20 ms, the period of time when both ECRH and sloshing beams were on. In these early experiments we were learning how to increase the central cell density by central cell gas puffing. Consequently the temporal behavior of the density was quite irregular. In the data shown here the central cell and plug densities are nearly equal. In other experiments shown in Fig. 9 we have obtained plugging with $n_c > n_p$. In these experiments we puffed additional gas into the central cell to buildup the central cell density. Central-cell ICRH probably created a nonisotropic ion distribution so that some of the density measured by the midplane microwave interferometer would not have penetrated into the mirror throats. In another shot without ICRH we also observed $n_c > n_p$. This is the first time that we have observed electrostatic confinement without having the end plug density above the central cell density. As mentioned in the Executive Summary, this is one of the distinguishing features of the thermal barrier concept.

When the ion end losses are so strongly reduced the ion end loss analyzer signal ion current could be canceled by current from electrons with energy sufficient to penetrate the 5-kV repeller. Consequently we can only estimate the axial confinement time to be 20 to 80 ms. At this time radial losses are most important, especially at the edge. The radial confinement time determined from net current collectors is 4 to 8 ms.

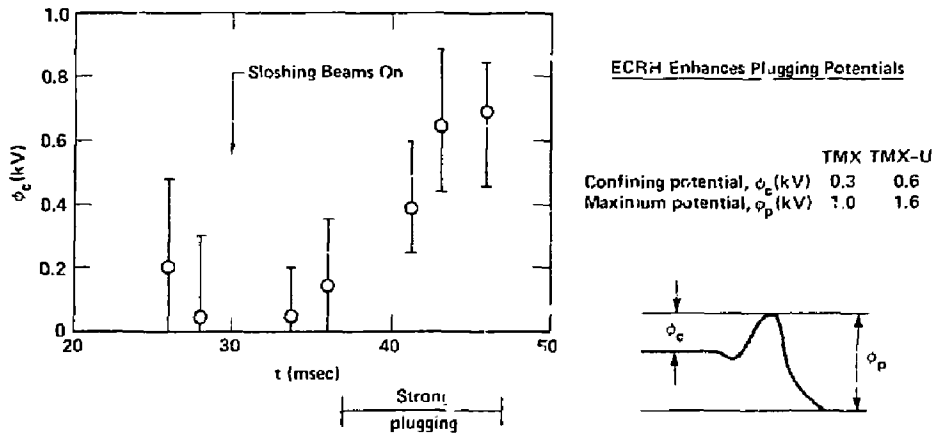

Figure 7. Measurements of plasma potential difference between west end plug and central cell. During strong end plugging a 0.4- to 0.7-kV confining potential is measured.

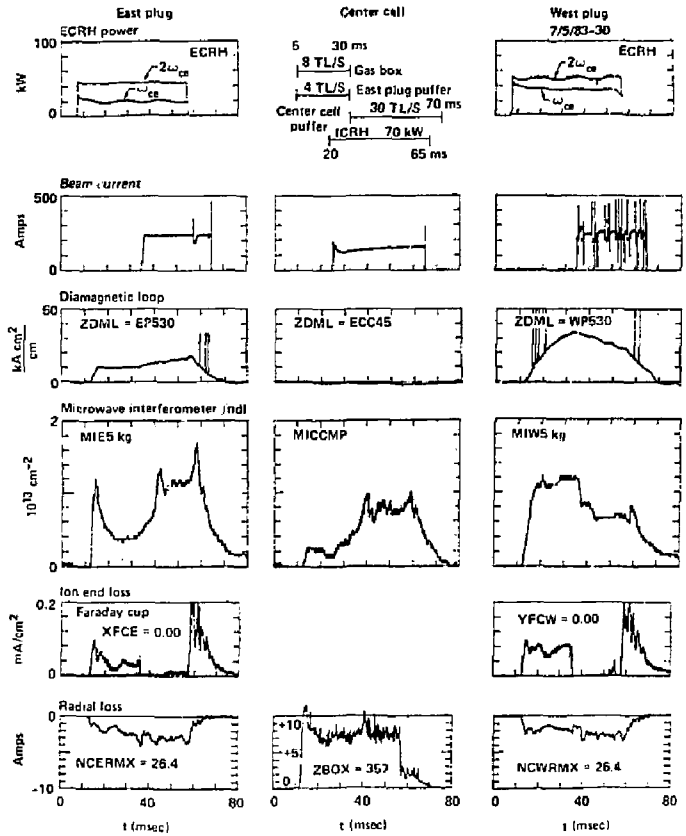

Figure 8. Measurements of end plugging on both ends for 20 ms. End plugging duration is limited by gyrotron pulse length. Shown are signals vs time in the east plug, central cell, and, west plug: (a) ECRH power, (b) beam power supply current, (c) diamagnetic loop, (d) microwave interferometer electron line density, (e) Faraday cup end loss current, and (f) radial loss current.

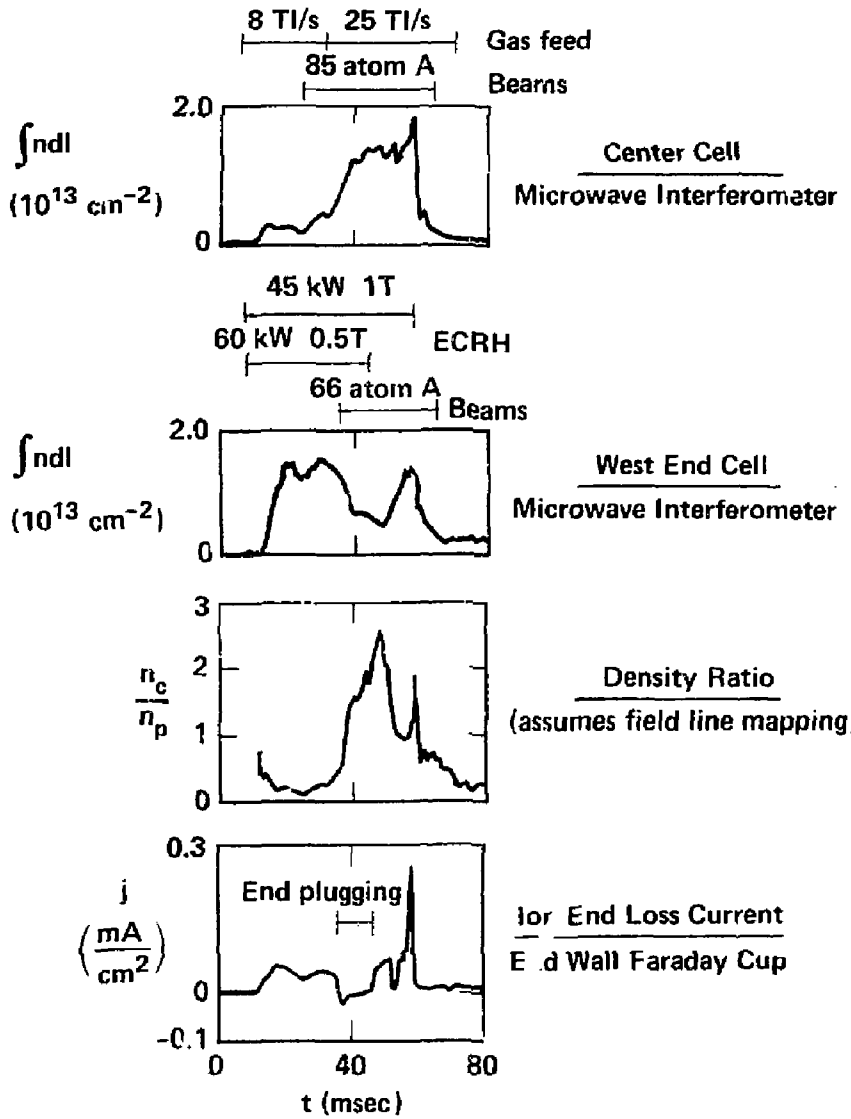

Figure 9. Experiments with central cell gas puffing show end plugging with $n_c > n_p$. Shown vs time is: (a) central cell line density, (b) west end cell line density, (c) central cell to plug density ratio, and (d) ion end loss current density. This shot (No. 21, July 5, 1983) had ICRH which may have helped increase the central cell density. However, shot 20 on the same day without ICRH showed a similar ratio between the central cell and west plug density.

Absolutely essential to the success of these experiments is the control of cold gas from neutral-beam injectors and wall reflux. Figure 10 shows the pressure measured by an ionization gauge in the west end plug and west end fan tank together with the ion end loss current density. First note that the end plug pressure maintains below 10^{-6} Torr during the discharge. In operation without adequate titanium gettering on the walls the pressure continued to rise and ultimately terminated the end plugging. The time history of pressure in the end fan tank gives further evidence for strong end plugging. The pressure buildup ceases when the end losses are terminated. This very global measurement indicates that the end plugging is occurring across the entire plasma radius and that the reduction in ion end losses is not an instrumental effect, such as that caused by hot electrons penetrating into the end wall diagnostic instruments.

An important feature of thermal barrier operation is that low-energy ions need to be pumped out of the potential depression. In TMX-U the sloshing beams are aimed at the midplane to charge-exchange away low-energy ions. To augment this process, and to limit the sloshing-ion density to below ECRH cutoff, TMX-U is equipped with pump beams at 18 deg with respect to the magnetic axis. Figure 11 demonstrates this charge-exchange pumping technique. Since pump beam ions are in the loss cone, they are not mirror-confined, and they have sufficient energy so that they are not potentially confined. Figure 11 shows that the density, plasma diamagnetism and sloshing-ion density indeed are reduced. The smaller change in total density indicates that the filling rate of low-energy ions is more rapid than the pump-out rate. The pump-out time constant is consistent with the predicted value. As the low-energy ions must also be pumped, we are developing (a) ICRH heating to reduce the collisional filling time of the warm ions, and (b) radial drift pumping as an alternative to charge exchange beam pumping.

IV. DISCUSSION

A remarkable feature of these end plugging experiments is that even with a plasma potential of 1.6 kV and without end losses to supply warm stabilizing ions, we did not observe any ion cyclotron fluctuations in the end cells. One explanation is that at the low plug densities of these experiments

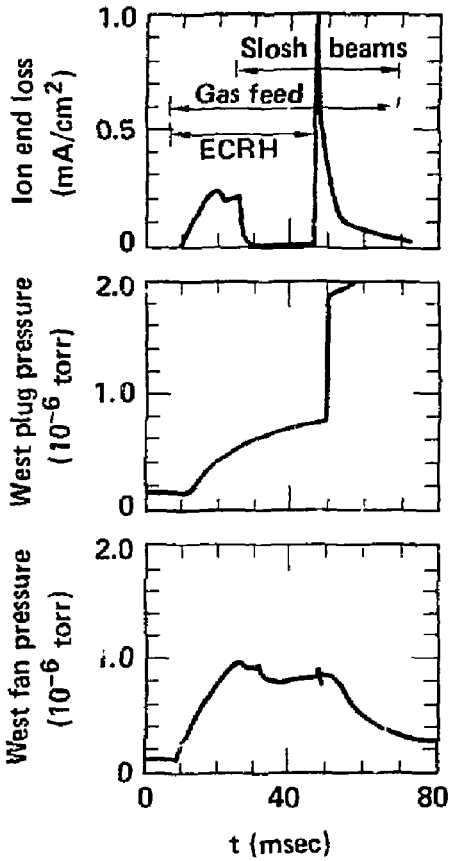

Figure 10. Measurements vs time of (a) the ion end losses, (b) plug region gas pressure and (c) end fan gas pressure.

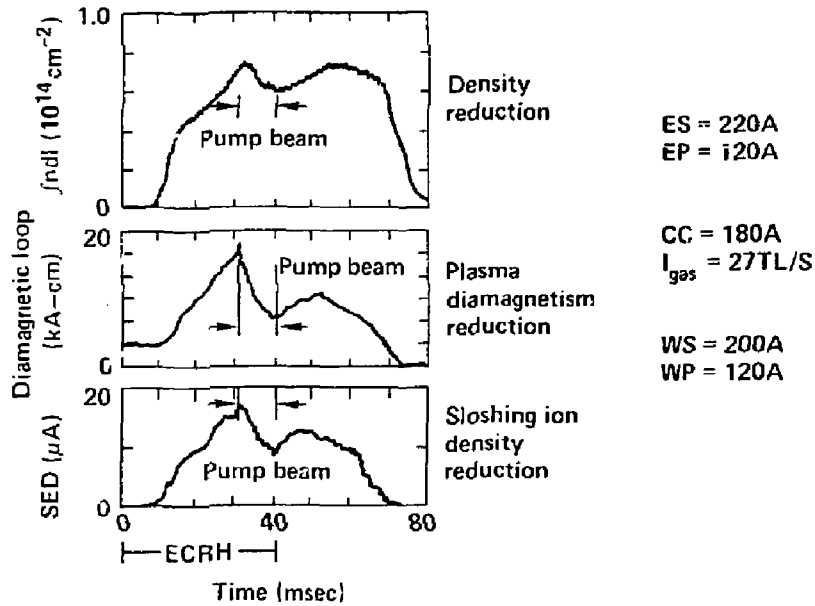

Figure 11. Demonstration of charge-exchange pumping technique on sloshing ions. Shown vs time is the (a) line density, (b) diamagnetic loop and, (c) the sloshing ion density. When the pump beam is on the sloshing-ion density is reduced.

(3×10^{11} cm^{-3}) the parallel wavelengths are long ($\lambda_{\parallel} \sim 3$ m) compared to the localized instability drive region. This region lies between the potential peak (peak of the sloshing-ion density) and the outboard mirror point where ion cyclotron fluctuations have previously [1,16] been observed during high density sloshing-ion experiments. Whether fluctuations develop at higher plug density (5×10^{12} cm^{-3}) and whether they remain benign is one of the central issues to be resolved in future TMX-U experiments.

Because of the strong axial plugging in these experiments, the dominant particle losses are due to radial transport. Work is currently underway to identify the as yet unknown mechanism. Previous measurements in high density, sloshing-ion plasmas showed that the dominant mechanism for radial losses was electric mobility due to charge-exchange collisions accompanying particle fueling.[18] Because the low fueling rates are adequate to fuel the present plasmas, this mechanism is small and accounts for only about 10% of the observed transport. Resonant (neoclassical) transport, predicted to be dominant in hot, high-density plasmas, is also small because of low collisionality. Additional mechanisms are being considered at this time, including transport due to low frequency oscillations. Such oscillations are observed during ECRH, but analysis of data has not demonstrated a correlation between them and the radial transport. Theoretically, however, oscillations could drive a radial flux. Future experiments are being planned to more thoroughly test hypotheses that this or other mechanisms are responsible for the observed transport.

In the Executive Summary of this report we noted that we have not yet made direct measurements of a thermal barrier potential dip. We can report, however, that the presence of a thermal barrier in TMX-U is consistent with the measured time histories of the plasmas in the plugs and central cell.

In a tandem mirror, the plasmas in the plugs and central cell can be strongly coupled because the central cell is the primary source of particles for the plugs. The ionization and charge-exchange of the sloshing ion beams with the trapped and passing ions from the central cell is the primary source of sloshing ions. The trapping and heating of central cell electrons that pass through the fundamental ECRH resonance is the primary source of the mirror confined electrons in the plugs. Without peaks and valleys in the axial potential profile, the plug density will tend to increase when the central cell density increases and decrease when the central cell density decreases.

Four axial potential profiles which may have been created in TMX-U are shown in Fig. 12. The first (case a) is a simple tandem with sloshing ions. Plugging is achieved only for $n_p > n_c$. The second profile (case b) is labelled "ECRH enhanced." This profile does not have a thermal barrier (the potential at the plug midplane does not dip below that of the central cell) so the central-cell electrons are essentially free to circulate through the fundamental ECRH resonance. However, the plugging potential is enhanced above that of a simple, sloshing-ion tandem (case a) because the ECRH distorts the plug electron distribution away from a Maxwellian. We also allow that a potential peak occurs at the sloshing ion turning point near the central-cell. This potential peak is caused by the sloshing ion density peak at their turning point.

Case c is a "Modified Thermal Barrier." This profile is different from Case d--the standard thermal barrier--because a potential peak occurs at the inner sloshing-ion turning point. This inner potential peak is important in both cases b and c because it helps isolate the plugs from the central cell ions by reducing the number of central cell ions that pass through the plug midplane. This reduces the target for the sloshing beams and reduces the barrier filling rate.

As noted in Fig. 12 each of these possible potential profiles would change the coupling between the plug and the central cell. These different potential profiles, therefore, may help to explain the different responses of the plug plasmas to the changes in the central cell density (Fig. 8) when the sloshing beams are turned on and the central cell gas fueling is increased.

As shown in Fig. 8, both ends of the device show strong plugging even though $n_p \approx n_c$. Therefore, we do not believe that either plug can be explained by a simple tandem potential profile (case a).

The fact that the east plug density increases as the central cell density increases shows that this plug and the central cell are still strongly coupled. For this reason we believe that the "ECRH Enhanced" potential profile was present in the east plug on this shot. This potential profile does not have a thermal barrier, so as the central cell density increased the number of electrons passing through the fundamental resonance increased. This increased the ECRH trapping rate for hot electron creation, which caused the east plug density and diamagnetism to increase as shown in Fig. 8.

Types of tandems		Plug characteristics
a. Simple	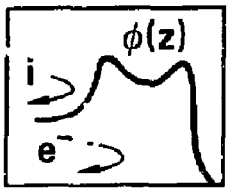	• Plugging for $n_p > n_c$.
b. ECRH enhanced	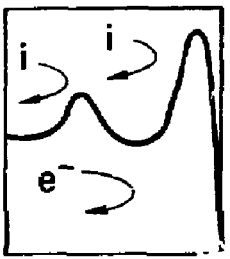	• ECRH target $\alpha\, n_c$ so $n_p \alpha\, n_c$.
c. Modified thermal barrier	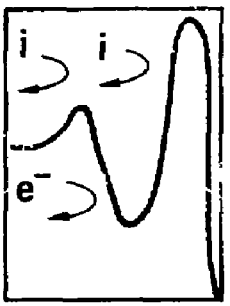	• ECRH target $\alpha\, n_c\, e^{-\phi_b/T_{ec}}$, so increasing ϕ_b may decrease n_p. Sloshing beam target limited by inner ϕ-peak. Allows $n_c \cong 2\, n_p$ w/o barrier filling.
d. Thermal barrier	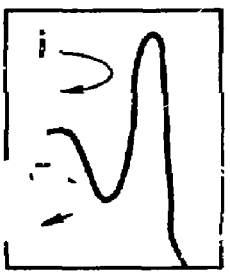	• ECRH target $\alpha\, n_c\, e^{-\phi_b/T_{ec}}$. Sloshing beam target $\alpha\, n_c$.

Figure 12. Various possible axial potential profiles. For the data of Fig. 8 the east plug is best described by (b) and the west plug by (c).

The west plug, however, had a higher density of hot electrons than did the east plug (based on the line density and diamagnetic loop signals - Fig. 8) before the sloshing-ion beams were turned on, so it is reasonable that a "modified thermal barrier" could be created in the west plug and not the east on this shot. With a modified thermal barrier, the plug is isolated from the central cell ions by the inner potential peak and from the central cell electrons by the thermal barrier. The isolation created by this potential profile explains why the west plug density actually decreased while the central cell density increased on this shot: the thermal barrier created by the pumping by the sloshing-ion beams exponentially reduced the number of electrons passing through ECRH resonance, thereby, reducing the source of hot electrons.

This same reduction of the plug density due to the turning on the plug beams could have occurred if the west plug potential profile was like case d--a standard thermal barrier. We believe, however, that the inboard potential peak of the modified thermal barrier is necessary to explain the data because we do not believe that our beam current was sufficient to pump a thermal barrier if all of the central cell ions were cold and able to trap in the barrier. In either case (c or d) a thermal barrier is required to explain the decoupling of the central cell and west plug.

From this analysis, therefore, we can say that the data is consistent with thermal barriers formed in TMX-U. We plan to make cooperative measurements of the potential profile this fall.

ACKNOWLEDGMENTS

It is a pleasure to thank the many people who contributed to the work described in this report: the engineering groups, technical operations teams, computer group, theoretical and experimental physics groups, and the Sandia Laboratory surface interaction group.

REFERENCES

[1] T. C. Simonen, S. L. Allen, T. A. Casper, J. F. Clauser et al., TMX-Upgrade (TMX-U) Operation in the Sloshing-Ion Mode, Lawrence Livermore National Laboratory, Livermore, CA, UCID-19568 (1982).

[2] B. W. Stallard, P. Poulsen, A. W. Molvik, W. E. Nexsen et al., Preliminary Analysis of the Initial TMX-U ECRH Results, Lawrence Livermore National Laboratory, Livermore, CA, UCID-19665 (1983).

[3] F. H. Coensgen, T. C. Simonen, A. K. Chargin, and B. G. Logan, TMX-Upgrade Major Project Proposal, Lawrence Livermore National Laboratory, Livermore, CA, LLL-Prop-172 (April 1980).

[4] D. E. Baldwin and B. G. Logan, "Improved Tandem Mirror Fusion Reactors", Phys. Rev. Lett. 43, 1318 (1979).

[5] D. L. Correll, S. L. Allen, T. A. Casper et al., "Ambipolar Potential Formation and Axial Confinement in TMX," Nucl. Fusion 22, 223 (1982).

[6] S. L. Allen, T. A. Casper, J. F. Clauser et al., Summary of Results from the Tandem Mirror Experiment (TMX), Lawrence Livermore National Laboratory, Livermore, CA, UCRL-53120 (1981).

[7] T. C. Simonen, "Experimental Progress in Magnetic--Mirror Fusion Research," Proc. IEEE, 1981, (IEEE Piscataway, NJ, 1981) 69, 935-957.

[8] T. K. Fowler and B. G. Logan, "Tandem Mirror Reactor," Comments Plasma Phys. Controlled Fusion 2, 167 (1977).

[9] G. I. Dimov, V. V. Zahaidahov, and M. E. Kishinevshii, "Thermonuclear Confinement System with Two Mirror Systems," Fiz. Plasmy 2, 597 (1976); [Sov. J. Plasma Phys. 2, 326 (1976)].

[10] G. A. Carlson, B. Arfin, W. L. Barr et al., Tandem Mirror Reactor with Thermal Barriers, Lawrence Livermore National Laboratory, Livermore, CA, UCRL-52836 (1979).

[11] T. A. Casper and G. R. Smith, "Observation of Alfven Ion Cyclotron Fluctuations in the End-Cell Plasma in the Tandem Mirror Experiment," Phys. Rev. Letters, 48, 1015 (1982).

[12] R. H. Cohen, Potentials in Thermal Barriers with Strong Electron Cyclotron Heating, Lawrence Livermore National Laboratory, Livermore, CA, UCRL-88939 (1983) (to be published in Phys. Fluids Lett.).

[13] Y. Matsuda and T. Rognlien, Numerical Solution of the Electron Distribution Function in Tandem-Mirror Thermal Barriers, Lawrence Livermore National Laboratory, Livermore, CA, UCRL-89124 (1983) (to be published in Phys. Fluids Lett.).

[14] A. W. Molvik and S. Falabella, Use of ICRH for Startup and Initial Heating of the TMX-U Central Cell, Lawrence Livermore National Laboratory, Livermore, CA, UCID-19342 (1982).

[15] B. W. Stallard, "Experiments on Hot-Electron ECRH in the Tandem Mirror Experiment-Upgrade," in 5th Topical Conference on RF Plasma Heating, Madison, Wisconsin, 1983 (University of Wisconsin, Madison, WI, 1983).

[16] T. C. Simonen, S. L. Allen, T. A. Casper et al., "Operation of the Tandem-Mirror Plasma Experiment with Skew Neutral-Beam Injection," Phys. Rev. Letters 50, 1668 (1983).

[17] T. J. Orzechowski et al. Measurements of Sloshing Ion Spatial Profiles in End Cell of Tandem Mirror Experiment-Upgrade (TMX-U), Lawrence Livermore National Laboratory, Livermore, CA, UCRL-88447 (1983) (to be published in Phys. Fluids Lett.).

[18] S. P. Auerbach, R. H. Cohen, J. M. Gilmore, E. B. Hooper, Jr., A. A. Mirin, and M. E. Rensink, Plasma Transport Caused by Ion-Neutral Atom Collisions, Lawrence Livermore National Laboratory, Livermore, CA, UCRL-89860 (1983).

4059v/CJ/mm